Supporting Information

Engineering of Mn_3O_4@Ag Microsphere Assembled by Nanosheets for Superior O_3 Decomposition

1 Catalyst Characterization and catalytic activity test

XRD (X-ray powder diffraction) patterns were collected on a Panalytical Aries X-ray diffractometer under Cu K_α radiation. The data were obtained at a scan speed of 5 (°)·min^{-1} from 10° to 80° with a step of 0.01°. The Raman spectra were obtained from a LabRAM HR800 UV Laser Raman spectrometer with a wavelength of 633 nm, with a power of 0.04 mW. FE-SEM (field emission scanning electron microscopy) was performed with electron microscopy (SU8220, Hitachi). HRTEM of the catalyst was performed on an FEI Themis Z instrument at 300 kV. N_2 adsorption-desorption experiments were performed with an Autosorb iQ2 (ANTON PAAR QUANTATEC INC) and all samples were degassed at 250 °C for 2 h at vacuum ambiance. Specific surface area was measured with the BET method, and average pore size distribution with the BJH method. The amount of Ag in Mn_3O_4 was measured on inductively coupled plasma light emission spectroscopy (Agilent 5110). H_2-TPR (hydrogen temperature-programmed reduction) and O_2-TPD (oxygen temperature-programmed desorption) experiments were conducted with the Micro. AutoChem Ⅱ 2920. During H_2-TPR, 30 mg of the sample were preprocessed in Ar at 110 °C for 0.5 h. After cooling to room temperature, it was heated to 600 °C in 5% H_2/Ar with a rate of 10 °C min^{-1}.

For O_2-TPD, 30 mg of catalyst was pretreated under He atmosphere at 110 °C for 30 min, and then cooled to room temperature, followed by exposing to O_2 for 30 min. Then, it was heated to 800 °C in flowing He. The signals were detected by TCD. Water desorption (H_2O-TPD-MS) measurement was performed on a Hiden catlab test instrument equipped with a mass spectrometer. The catalyst was heated to 110°C under Ar and kept for 0.5 h to remove the adsorbed water and cooled to room temperature (30°C). Then saturated water (30°C) was introduced by Ar (40mL min^{-1}) for 1 h; The supersaturated adsorbed water was removed by Ar. Finally, the catalyst was heated from 30°C to 600 °C, and the desorption signals were detected: 32(O_2), 18(H_2O), 44(CO_2), 28(CO or N_2). XPS (X-ray photoelectron spectroscopy) data was acquired with an VG MultiLab 2000 device employing an MgK_α source. Thermogravimetric testing (TG) was performed on a thermogravimetric analyzer (NETZSCH STA449F5). The test conditions are: nitrogen atmosphere, heating at a rate of 10 °C min^{-1}.

The catalytic activity was evaluated in a fixed-bed continuous flow reactor (8 mm inner diameter). 20 mg of catalyst was packed into the reactor at a gas hourly space velocity (GHSV) of 600 L g^{-1} h^{-1}. During the test, the temperature was maintained at 25°C and the relative humidity (RH) of the feed gas was maintained at 50%. Ozone was generated by a vacuum ultraviolet lamp, and the inlet and outlet ozone concentrations were analyzed using an ozone detector (Model 106-L, 2B Technologies, USA). The ozone conversion was calculated by the following equation:

$$O_3 \text{ conversion} = (C_{in} - C_{out}) / C_{in} \times 100\%$$

where C_{in} and C_{out} are the inlet and outlet concentration of ozone, respectively.

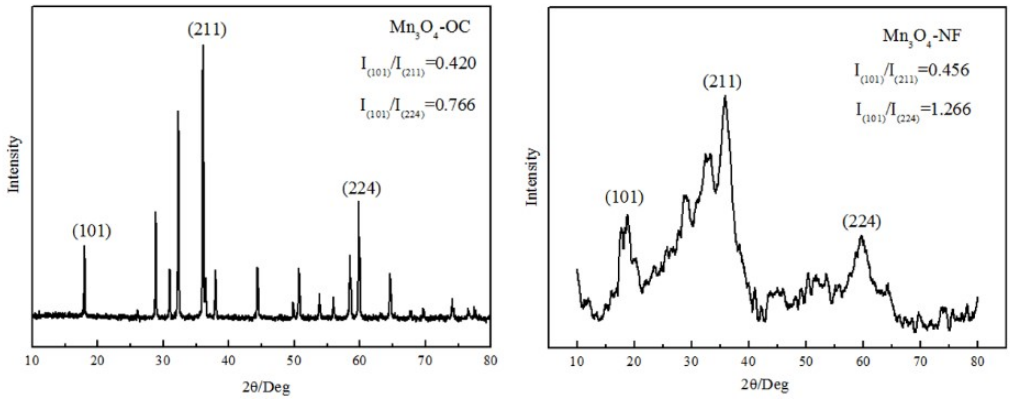

Fig.S1 Compare of XRD patterns of Mn_3O_4-OC and Mn_3O_4-NF

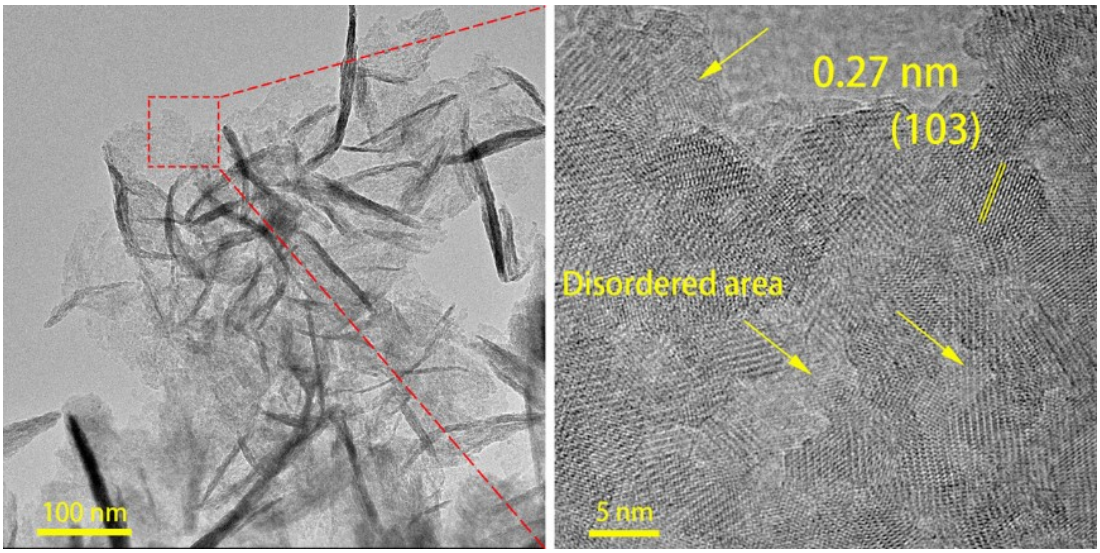

Fig.S2 the HRTEM image of Mn_3O_4-NF

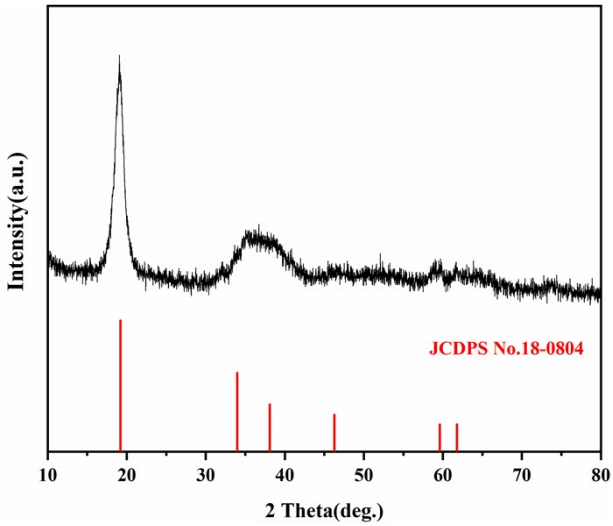

Fig.S3 the XRD pattern of the precursorβ-MnOOH

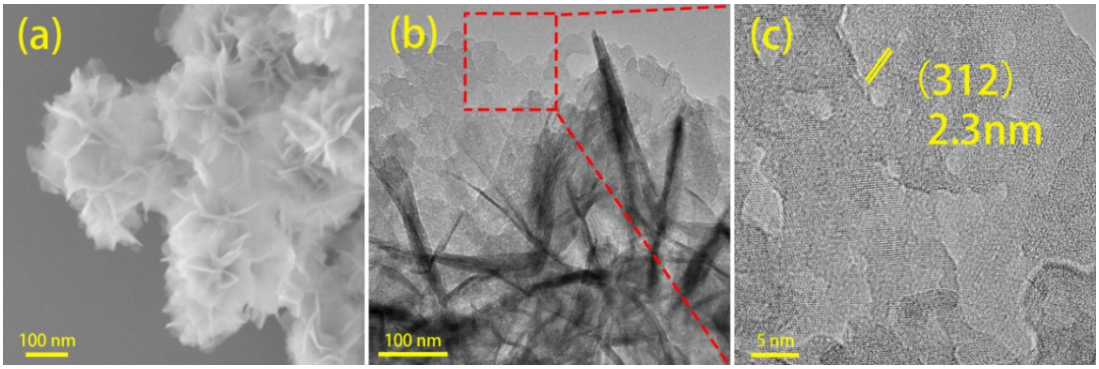

Fig.S4 the SEM (a) and HRTEM (b) image of the precursor β-MnOOH

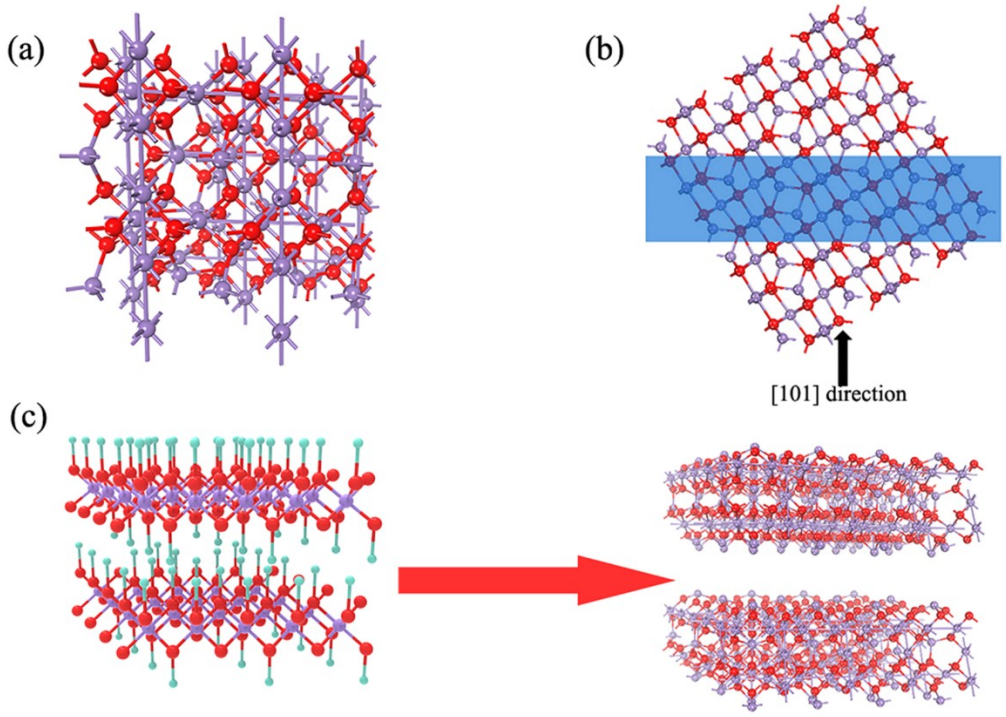

Fig.S5 Crystal structure of bulk Mn_3O_4. (b) Side-view of Mn_3O_4 along b axis. (c) Schematic diagram of topochemical conversion from β-MnOOH nanosheets to Mn_3O_4 nanosheets.

（the CIF file of β-MnOOH can not be found from the CrystallographyOpen Data website, its structure is referenced as reported in : Inorg. Chem. 2000, 39, 741 ）

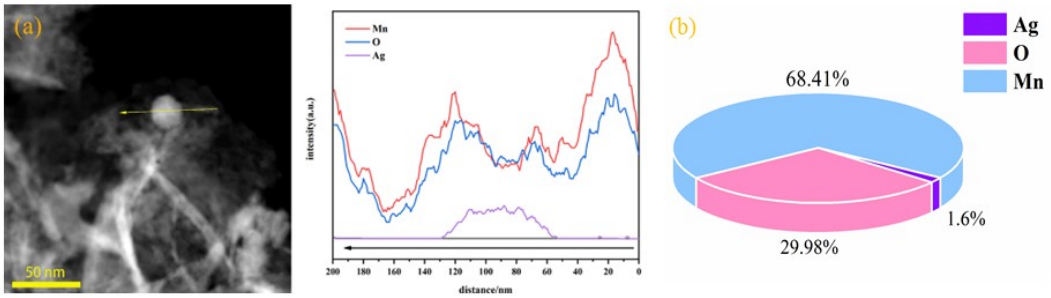

Fig.S6 the line-mapping of Ag@Mn_3O_4-NF(a) and ICP-OES result (b)

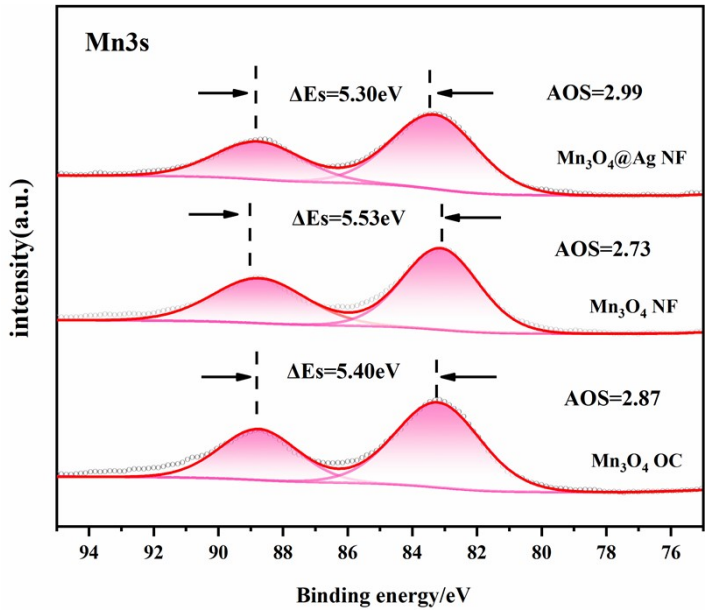

Fig.S7 the Mn3s spectra of Mn_3O_4-OC, Mn_3O_4-NF and Mn_3O_4@Ag-NF (AOS=8.956-1.126ΔEs)

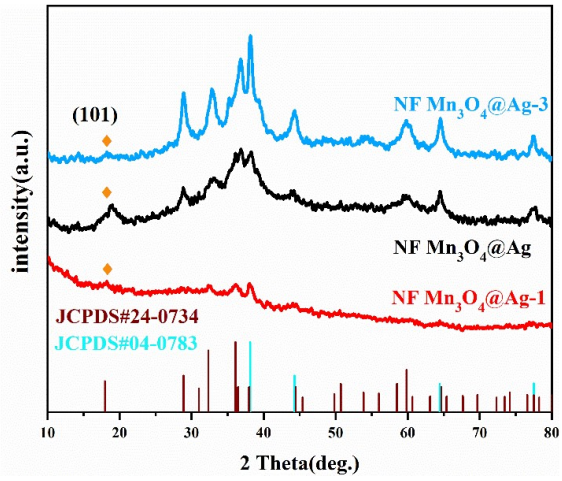

Fig. S8 the XRD patterns of Mn_3O_4@Ag-NF(1), Mn_3O_4@Ag-NF and Mn_3O_4@Ag-NF(3)

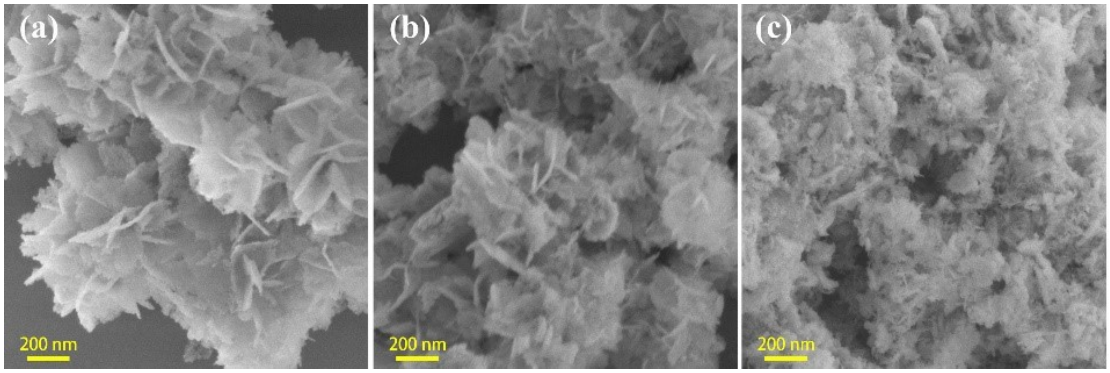

Fig. S9 SEM images of Mn_3O_4@Ag-NF(1)(a), Mn_3O_4@Ag-NF(b) and Mn_3O_4@Ag-NF(3) (c)

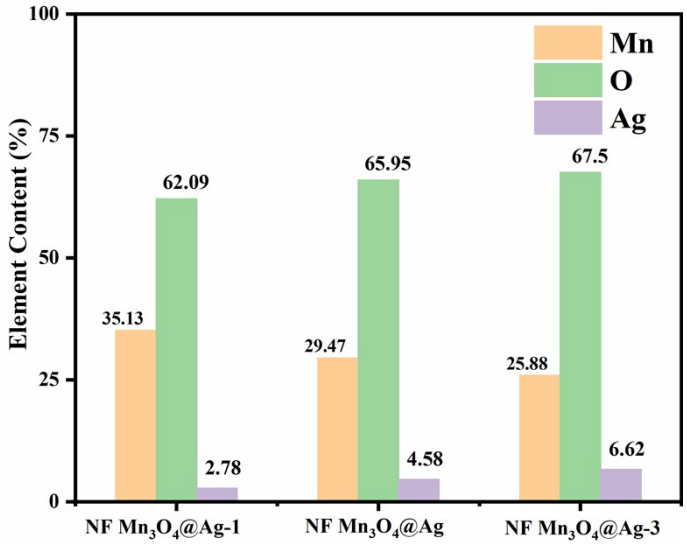

Fig. S10 The EDX of Mn_3O_4@Ag-NF(1), Mn_3O_4@Ag-NF and Mn_3O_4@Ag-NF(2)

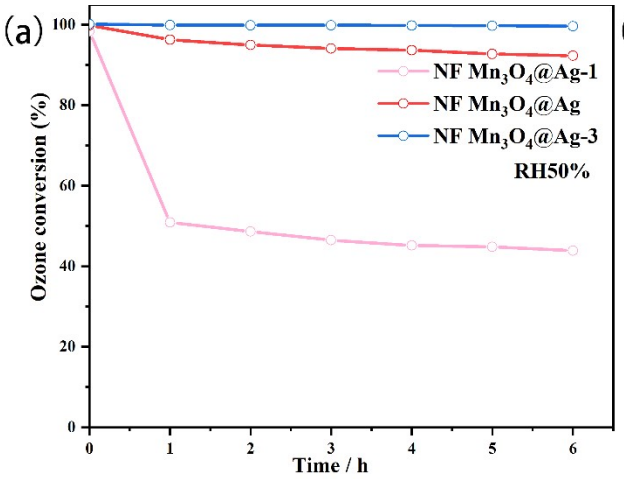

Fig.S11 Conversion of O_3 over Mn_3O_4@Ag-NF(1), Mn_3O_4@Ag-NF and Mn_3O_4@Ag-NF(3)

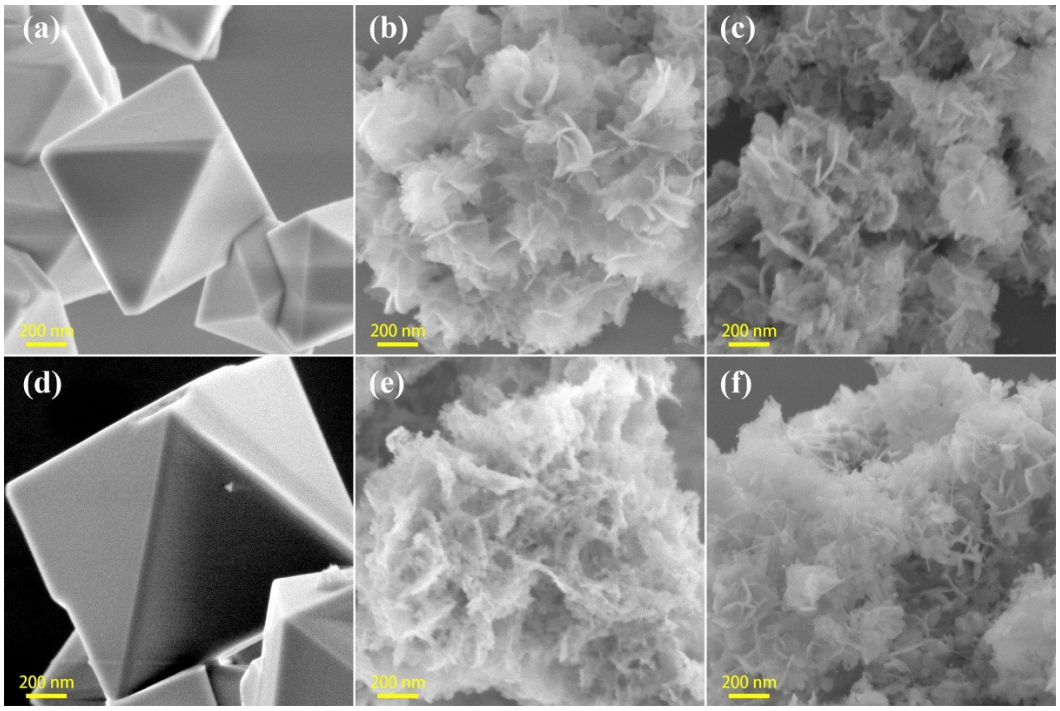

Fig. S12 SEM images before test: Mn_3O_4-OC(a), Mn_3O_4-NF(b) and Mn_3O_4@Ag-NF(c) and SEM images after test: Mn_3O_4-OC(d), Mn_3O_4-NF(e) and Mn_3O_4@Ag-NF(f)

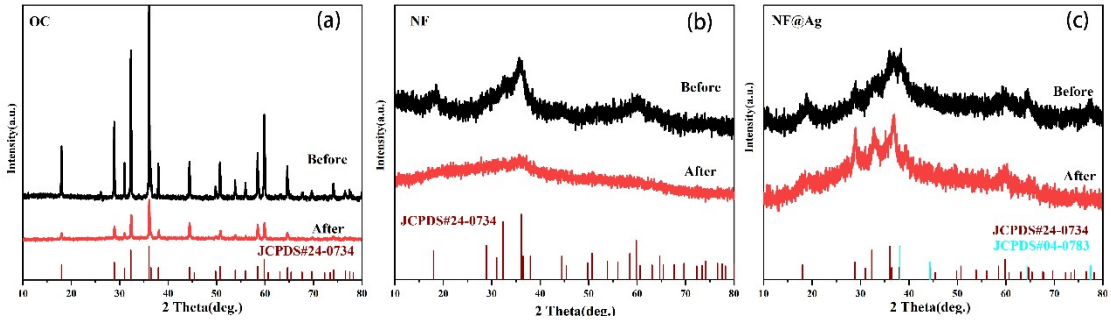

Fig. S13 The XRD before and after test: Mn_3O_4-OC(a), Mn_3O_4-NF(b) and Mn_3O_4@Ag-NF(c)

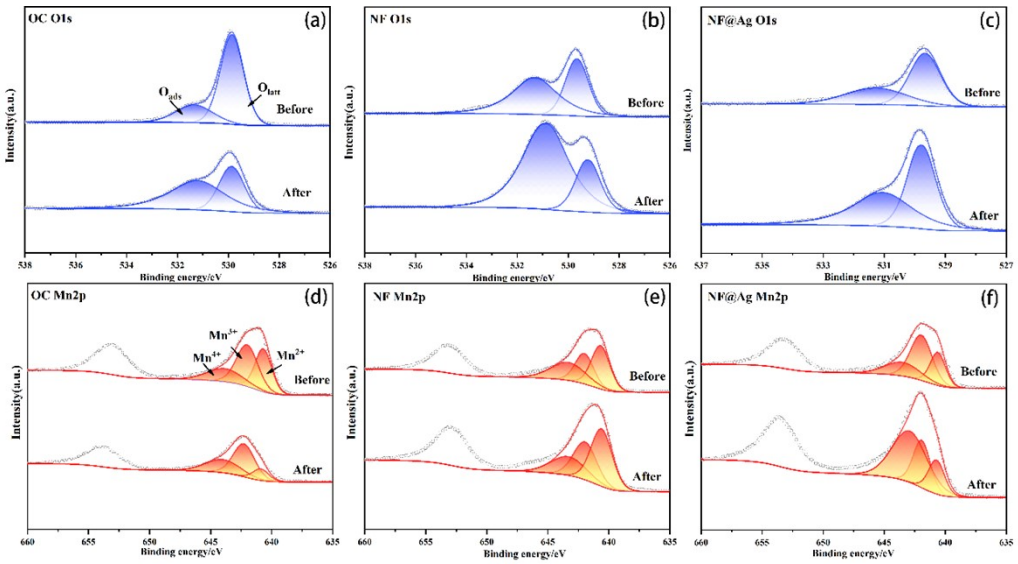

Fig. S14 XPS spectra of the fresh (marked as before) and used (marked as after) Mn_3O_4-OC, Mn_3O_4-NFand Mn_3O_4@Ag-NF: (a,b,c)O1s;(d,e,f)Mn2p

Table S1 the O_3 decomposition performance over reported MnOx based catalysts

Catalyst	O_3 Con./ppm	Catalyst amount/mg	WHSV L g^{-1} h^{-1}	RH	Activity after 6h
Mn_3O_4-NF	20	100	600	50	57%
Mn_3O_4@Ag-NF (This work)	20	100	600	50	92.5%
Mn_3O_4[1]	15	100	600	50%	~35%
Fe-MnOx[2]	100	100	660	60	~73%
Ce-MnO_2[3]	50-60	50	300	Dry gas	＜80%
Ce-MnO_2[4]	40	100	600	45%	~97%
MnO_2@GR[5]	50	100	540	50	~72%
Amorphous MnO_2[6]	20	100	600	50	100%
Li-K-OMS-2[7]	45	100	660	60	~92%
Ce-α/γ-MnO_2[8]	45	100	300	65	98%
α-MnO_2[9]	23	unknown	880	45	<60%
Ce-OMS-2[10]	40	100	600	45	~100%
Co-OMS-2[10]	40	100	600	45	~70%
Fe-OMS-2[10]	40	100	600	45	~55%

Table S2 the chemical properties of used catalysts based on XPS

Sample	Content (%)			O_{ads}/O_{latt}
	Mn^{2+}	Mn^{3+}	Mn^{4+}	
Mn_3O_4-OC	14.07	50.25	35.68	1.56
Mn_3O_4-NF	21.2	50.51	28.29	3.22
Mn_3O_4@Ag-NF	25.48	35.91	38.61	0.96

Reference

1. L. Zhang, S. Wang, L. Lv, Y. Ding and D. Tian, *Langmuir*, 2021, 37, 1410-1419.
2. J. B. Jia, W. J. Yang, P. Y. Zhang and J. Y. Zhang, *Appl. Catal. A*, 2017, 546, 79-86.
3. Y. Liu and P. Y. Zhang, *Appl. Catal. A*, 2017, 530, 102-110.
4. L. Yang, J. Ma, X. Li, G. He, C. Zhang and H. He, *J. Environ. Sci. (China)*, 2020, 87, 60-70.
5. G. Zhu, W. Zhu, Y. Lou, J. Ma, W. Yao, R. Zong and Y. Zhu, *Nat. Commun.*, 2021, 12, 4152.
6. S. Liu, J. Ji, Y. Yu and H. Huang, *Catal. Sci. Techno.*, 2018, 8, 4264-4273.
7. W. Hong, J. Z. Ma, T. L. Zhu, H. He, H. N. Wang, Y. Sun, F. X. Shen and X. Li, *Appl. Catal. B*, 2021, 297, 120466.
8. X. Li, J. Ma, C. Zhang, R. Zhang and H. He, *J. Environ. Sci. (China)*, 2020, 91, 43-53.
9. J. Jia, P. Zhang and L. Chen, *Catal. Sci. Technol.*, 2016, 6, 5841-5847.

10. J. Z. Ma, C. X. Wang and H. He, *Appl. Catal. B*, 2017, 201, 503-510.